



Influence of the interphase zone on the nanoparticle debonding stress

Michele Zappalorto, Marco Salviato, Marino Quaresimin *

University of Padova, Department of Management and Engineering, Stradella S. Nicola 3, 36100 Vicenza, Italy

ARTICLE INFO

Article history:

Received 1 January 2011

Received in revised form 15 September 2011

Accepted 27 September 2011

Available online 2 October 2011

Keywords:

A. Nano particles

B. Debonding

B. Interphase

B. Interfacial strength

ABSTRACT

One of the most appealing features concerned with nanomodification of polymeric resins for structural applications is the perspective of obtaining high toughness even at low nanofiller volume fractions. Such performances are related to the energy dissipated through the damage mechanisms taking place at the nanoscale. Among these, nanoparticle debonding could take an important role either as a mechanism itself or as a trigger for phenomena like plastic void growth or matrix shear yielding. In the present work, a model for the hydrostatic tension related to debonding is presented. The model accounts for some important issues inherently related to the nanoscale with particular reference to the emergence of an interphase surrounding the nanoparticle. Results can be useful in view of a multi-scale modelling of the problem.

© 2011 Elsevier Ltd. All rights reserved.

1. Introduction

In the recent literature great attention has been paid to nanoscale reinforcements to significantly increase polymer stiffness, strength and toughness with low reinforcement concentrations (see, among the others, [1–6]). The improvement of polymer toughness broadens the nanocomposite field of standalone applications and makes the use of nanocomposite systems as matrices for fibre reinforced composites a smart solution. As a matter of facts, nanomodified polymers can be the basis for the further development of a new class of composites through which all the benefits coming from nanosized materials together with all those concerned with the addition of micrometric size fibres can be synergistically exploited.

The understanding of the relation between the nanostructure and the overall mechanical behaviour of nanocomposites plays an important role in the development of such materials. This need has given rise in the literature to a large number of modelling strategies. Thostenson and Chou [7] proposed a model for an epoxy matrix reinforced by aligned multi-walled carbon nanotubes (MWCNTs), where the actual filler nanostructure is accounted for by introducing a solid effective fibre through an iso-strain condition.

Independently, Luo and Daniel [8] studied the prediction of elastic properties of polymer layered silicate (PLS) nanocomposites. They accounted for the nanoclay morphology by a three-phase Mori-Tanaka model (matrix, exfoliated clays and cluster of intercalated

clays) and for the actual nanofiller orientation and grade of exfoliation.

Recently, molecular modelling strategies based on discrete computational modelling techniques have also been used to investigate nanocomposite systems [9–13].

Different from the above mentioned works, which are focused on the assessment of elastic properties and disregard strengthening and toughening mechanisms, a study on the effects of nanoparticles on fracture properties of epoxy resins has been carried out by Wetzel et al. [14]. Together with a comprehensive experimental analysis, the authors studied the effects of various fracture mechanisms, such as crack deflection and crack pinning, by means of some micromechanical models. A similar approach has been later used by Johnsen et al. [15] and Zhao et al. [16].

A study on the energy dissipation due to the interfacial debonding of nanoparticles has been done by Chen et al. [17]. By means of an energy analysis of the process, these authors derived a simple size-dependent formulation for the debonding stress later used to compute the energy dissipation due to this mechanism. The size distribution of particles was thought of as obeying a logarithmic normal distribution and the Weibull distribution function was used to describe the probability of debonding at the interface.

More recently Lauke [18] analysed the energy dissipation phenomena by considering, besides particle debonding, voiding and subsequent yielding of the polymer. The conclusions drawn by Lauke are different depending on the used debonding criterion (critical stress or critical energy). The same author also provided the theoretical basis for a test to determine the interfacial adhesion strength between a coated particle and a polymer matrix material [19].

* Corresponding author. Tel.: +39 0444 998723; fax: +39 0444 998888.

E-mail address: marino.quaresimin@unipd.it (M. Quaresimin).

Williams [20] analysed in detail the toughening of particle filled polymers assuming that plastic void growth around debonded or cavitated particles is the dominant mechanism for energy dissipation.

All the works mentioned above are founded on the definition of a criterion for discriminating debonding. This particular problem was initially investigated by Nicholson [21], who considered a rigid spherical inclusion embedded in and completely adhered to a much larger sphere of matrix. Assuming that the adhesive bond was weak and the matrix sphere is subjected to a uniform fixed radial stress on its outer surface, Nicholson found a criterion for detachment. The case of a rigid spherical inclusion under a tensile stress applied to the elastomeric matrix was analysed by Gent [22]. Here the inclusion is assumed to have an initially-debonded patch on its surface and the conditions for growth of the patch are derived from fracture energy considerations.

In the previous works, the existence of only two different phases (i.e. the particle and the matrix) is assumed. Although this sounds reasonable at the microscale, it does not hold valid for nanosized reinforcements. In this case the molecular structure of the polymer matrix is significantly altered at the particle/matrix interface and this perturbed region is comparable in size with that of the nanoparticle [10,13]. In the present paper particular attention is paid to the interphase zone surrounding the nanoparticle, which, due to inter and supra-molecular interactions, might be characterised by chemical and physical properties different from those of the constituents. The aim of the present study is to determine a closed form expression for the critical debonding stress accounting for the existence of an interphase zone of different properties between the nanoparticle and the matrix. In more details:

- the problem is formulated and solved by considering a nanoparticle of radius r_0 surrounded by a shell-shaped interphase of radius a ;
- the expression for the critical debonding stress is determined within the frame of the Finite Fracture Mechanics (FFM) approach. Stress and displacement fields at incipient debonding and after debonding has taken place are determined by using the Cauchy Continuum Theory;
- the solution makes explicit the role played by the properties and the size of the interphase zone.

2. Description of the system under analysis

Different from traditional microsized composites, in nanoscale materials and structures, the surface effects become significant [23–25], due to the high surface/volume ratio. Then, as stated by Ajayan et al. [25], when dealing with polymer nanocomposites it is extremely important to analytically describe the presence of an interphase and to be able to correctly estimate properties accounting for the interfacial region [25].

Unfortunately, the data available so far in the literature about the interphase zone are not enough to precisely formulate the law of variation of its properties across the thickness, as well as its size. Those parameters varies from case to case [26]. For example, Odegard et al. [10], by using molecular dynamics (MD) simulations, studied a system made of silica nanoparticles and a polyimide matrix reporting the existence of an interphase zone whose size was comparable with that of nanoparticles and the elastic properties lower than those of the matrix. Different results have been obtained by Yu et al. [13]; these authors, studying systems made of epoxy resins, found an interphase zone stiffer than the matrix.

For the sake of simplicity, in this work we assume that, even if there might be a gradual transition of the interphase properties

across its thickness to the bulk ones, a through-the-thickness average is representative of the overall property distribution (according to [10,13]). Consequently, the interphase is supposed to be homogeneous and isotropic. Thus the system under investigation, shown in Fig. 1, is constituted by:

- a spherical nanoparticle of radius r_0 ;
- a shell-shaped interphase of external radius a and uniform properties;
- a matrix of radius b loaded by a hydrostatic stress S .

The properties required by the analysis can be computed by means of numerical simulations carried out within the frame of MD as done in [10,13]; such method provides, as outputs, the radial extension of the interphase as well as the elastic properties averaged through the interphase thickness.

The interphase extension might also be measured through the experimental approach proposed by Zammarrano et al. [27] even though it needs to be validated for nanofillers different from those considered by the authors.

3. An energy approach to the problem

According to the Finite Fracture Mechanics (FFM) approach [28], the debonding of a nanoparticle can be assessed by imposing the following energy and stress conditions:

$$-\frac{\delta U}{\delta A} \geq \gamma \quad \text{and} \quad \sigma \geq \sigma_c \quad (1a-b)$$

where σ_c is the normal interfacial strength, δU is the change in potential energy, δA is the newly created debonded surface and γ is the interfacial fracture energy.

With the aim to determine the critical debonding stress from Eq. (1a), it is possible to make use of the following equilibrium equation, involving the energy states of the system during the debonding process:

$$\delta W = \delta K + \delta U^{m+a} + \delta U^p + 4\gamma\pi r_0^2 \quad (2a)$$

where δW is the work done by external forces, δK is the variation in the kinetic energy, δU is the variation in the elastic energy stored in the matrix and interphase (δU^{m+a}) and in the nanoparticle (δU^p) and r_0 is the nanoparticle radius.

Since the initial state is static, δK is always positive and Eq. (2a) can be also rewritten as:

$$\delta W \leq \delta U^{m+a} + \delta U^p + 4\gamma\pi r_0^2 \quad (2b)$$

The term δW in Eq. (2b) can be expressed as:

$$\delta W = S \times \delta u^m(b) \times 4\pi b^2 \quad (3)$$

where $b \gg r_0$ represents the matrix radius, δu^m is the variation in the matrix displacement field from the initial condition (incipient

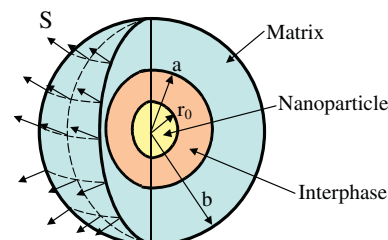


Fig. 1. Description of the system under analysis: nanoparticle of radius r_0 embedded in an interphase region of radius a . Bulk material of radius b subjected to a hydrostatic stress S .

debonding) to the final condition (post debonding) and S is the remotely applied hydrostatic stress which is not supposed to change during the debonding process (see Fig. 1).

At the same time, Clapeyron's theorem [29] guarantees that:

$$\begin{aligned}\delta U^p &= -\frac{1}{2} \sigma_{cr} \times \delta u^p(r_0) \times 4\pi r_0^2 \\ \delta U^{m+a} &= -\frac{1}{2} \sigma_{cr} \times \delta u^a(r_0) \times 4\pi r_0^2 + S \times \delta u^m(b) \times 4\pi b^2\end{aligned}\quad (4)$$

In Eq. (4) the terms δu^i represent the variation in the displacement fields from the initial condition (incipient debonding) to the final condition (post debonding).

It is then evident that the problem is translated into a stress analysis of the system at two different states: incipient debonding and post debonding. Moreover, Eq. (4) allows the energy condition given by Eq. (1a) to be rewritten as a stress condition.

4. Stress analysis

Displacement and stress fields can be determined within the frame of the Cauchy Continuum Theory regarding constituents as isotropic materials, in agreement with some recent works about nanocomposites [17,26,30].

The spherical symmetry of the problem (Figs. 1 and 2) guarantees that only the radial displacement u is nonzero, being it also independent of the angular coordinates θ and α .

Substituting stresses in terms of displacements into equilibrium equations and accounting for the spherical symmetry results in the following Euler equation for u :

$$\frac{d^2u}{dr^2} + \frac{2}{r} \frac{du}{dr} - \frac{2u}{r^2} = 0 \quad (5)$$

General solutions of Eq. (5) are:

$$u^m = A_m r + \frac{B_m}{r^2} \quad r \in (a, b] \quad \text{in the matrix} \quad (6)$$

$$u^a = A_a r + \frac{B_a}{r^2} \quad r \in (r_0, a] \quad \text{in the interphase} \quad (7)$$

$$u^p = A_p r + \frac{B_p}{r^2} \quad r \in [0, r_0] \quad \text{in the nanoparticle} \quad (8)$$

Accordingly, the radial stress components turn out to be:

$$\sigma_{rr,k} = 3K_k A_k - 4 \frac{B_k G_k}{r^3} \quad \text{with } k = m, a, p \quad (9)$$

where $K_k = E_k/[3(1 - 2\nu_k)]$ and $G_k = E_k/[2(1 + \nu_k)]$ are the bulk and the shear moduli of the k -th sub-dominion respectively.

It is noteworthy that the explicit expression of displacement and stress fields requires six constants to be determined. Since

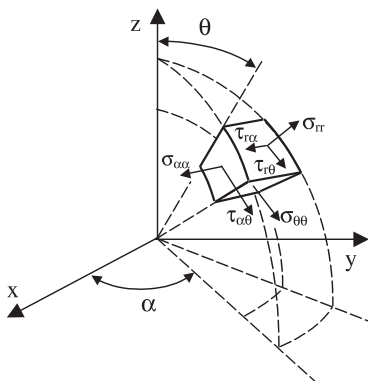


Fig. 2. Spherical coordinates system and stress components used to address the problem.

we are analysing two different states of the system, namely "incipient debonding" ("id") and "post debonding" ("pd"), the problem can be solved by determining twelve constants.

5. Stress and displacement fields at incipient debonding

At the condition of "incipient debonding" ("id"), displacement singularities in the particle can be avoided if and only if $B_p^{(id)} = 0$.

Assuming that debonding occurs when the radial stress around the particle reaches a critical value, σ_{cr} , boundary conditions for the problem can be written in terms of equilibrium and compatibility conditions as follows:

$$\sigma_r^p|_{r=r_0} = \sigma_{cr} \quad \sigma_r^a|_{r=r_0} = \sigma_{cr} \quad \sigma_r^a|_{r=a} = \sigma_r^m|_{r=a} \quad \sigma_r^m|_{r=b} = S \quad (10a-d)$$

$$u^p|_{r=r_0} = u^a|_{r=r_0} \quad u^a|_{r=a} = u^m|_{r=a} \quad (11a-b)$$

5.1. Displacement field within the nanoparticle

Substituting $B_p = 0$ into Eq. (8) and differentiating by r results in:

$$\varepsilon_r^p = \frac{du}{dr} = A_p^{(id)} \quad (12)$$

Moreover the nanoparticle is subjected to a hydrostatic stress field:

$$\sigma_r^p = \sigma_\theta^p = \sigma_z^p = \sigma_{cr} \quad (13)$$

Thus:

$$A_p^{(id)} = \frac{\sigma_{cr}}{3K_p} \quad (14)$$

Finally, substituting $A_p^{(id)}$ into Eq. (8):

$$u^p = \frac{\sigma_{cr}}{3K_p} r \quad (15)$$

5.2. Stress and displacement fields within the interphase

Coupling Eqs. (10b) and (11a) results in the following algebraic system:

$$\begin{cases} \sigma_{cr} = 3K_a A_a^{(id)} - 4 \frac{B_a^{(id)} G_a}{r^3} \\ \frac{\sigma_{cr}}{3K_p} r_0 = A_a^{(id)} r_0 + \frac{B_a^{(id)}}{r_0^2} \end{cases} \quad (16)$$

which, solved in $A_a^{(id)}$ and $B_a^{(id)}$, gives:

$$\begin{aligned} A_a^{(id)} &= \sigma_{cr} \frac{3K_p + 4G_a}{3K_p(3K_a + 4G_a)} \\ B_a^{(id)} &= \sigma_{cr} \frac{K_a - K_p}{K_p(3K_a + 4G_a)} r_0^3\end{aligned} \quad (17)$$

Then, stress and displacement fields can be expressed as a function of the normal stress acting on the nanoparticle, σ_{cr} :

$$\begin{aligned}\sigma_r^a &= \sigma_{cr} \frac{K_a(3K_p + 4G_a) - 4G_a(K_a - K_p)(\frac{r_0}{r})^3}{K_p(3K_a + 4G_a)} \\ u^a &= \frac{\sigma_{cr}}{K_p} r \left[\frac{3K_p + 4G_a}{3(3K_a + 4G_a)} + \frac{K_a - K_p}{(3K_a + 4G_a)} (\frac{r_0}{r})^3 \right]\end{aligned} \quad (18)$$

5.3. Stress and displacement fields within the matrix

Coupling Eqs. (10c) and (11b) results in the following algebraic system:

$$\begin{cases} 3K_a A_a^{(id)} - 4 \frac{B_a^{(id)} G_a}{a^3} = 3K_m A_m^{(id)} - 4 \frac{B_m^{(id)} G_m}{a^3} \\ A_a^{(id)} a + \frac{B_a^{(id)}}{a^2} = A_m^{(id)} a + \frac{B_m^{(id)}}{a^2} \end{cases} \quad (19)$$

which, omitting some algebraic manipulations, provides:

$$\begin{aligned} A_m^{(id)} &= \frac{\sigma_{cr}}{3K_p} \frac{(3K_a + 4G_m)(3K_p + 4G_a) + 12(K_a - K_p)(G_m - G_a)(\frac{r_0}{a})^3}{(3K_a + 4G_a)(3K_m + 4G_m)} \\ B_m^{(id)} &= \frac{\sigma_{cr}}{K_p} \frac{3K_p + 4G_a}{3K_a + 4G_a} \frac{K_m - K_a}{3K_m + 4G_m} a^3 + \frac{\sigma_{cr}}{K_p} \frac{3K_m + 4G_a}{3K_m + 4G_m} \frac{K_a - K_p}{3K_a + 4G_a} r_0^3 \end{aligned} \quad (20)$$

The relation between the boundary stress S and the normal stress at the interface σ_{cr} can be expressed as:

$$S = C_h \sigma_{cr} \quad (21)$$

where C_h is the reciprocal of the hydrostatic component of the *Global Stress Concentration Tensor* of the problem (see Appendix A).

Substituting Eq. (21) into the condition $\sigma_r^m|_{r=b} = S$ results in:

$$C_h = \frac{K_m}{K_p} \zeta \quad (22)$$

where

$$\begin{aligned} \zeta &= \frac{(3K_a + 4G_m)(3K_p + 4G_a)}{(3K_a + 4G_a)(3K_m + 4G_m)} + 12 \\ &\times \frac{(K_a - K_p)(G_m - G_a)}{(3K_a + 4G_a)(3K_m + 4G_m)} \left(\frac{r_0}{a}\right)^3 + 4 \frac{G_m}{K_m} \frac{3K_m + 4G_a}{3K_m + 4G_m} \\ &\times \frac{K_p - K_a}{3K_a + 4G_a} \left(\frac{r_0}{b}\right)^3 + 4 \frac{G_m}{K_m} \frac{3K_p + 4G_a}{3K_m + 4G_m} \frac{K_a - K_m}{3K_m + 4G_m} \left(\frac{a}{b}\right)^3 \end{aligned} \quad (23)$$

6. Stress and displacement fields after debonding

After debonding (“pd” state), the nanoparticle becomes unloaded and its displacement field is trivially zero. Then, only the following four boundary conditions are needed to solve the problem:

$$\sigma_r^a|_{r=r_0} = 0 \quad \sigma_r^a|_{r=a} = \sigma_r^m|_{r=a} \quad \sigma_r^m|_{r=b} = S \quad u^a|_{r=a} = u^m|_{r=a} \quad (24a-d)$$

Eqs. (24) lead to the following linear system:

$$\begin{cases} 3K_a A_a^{(pd)} - 4 \frac{B_a^{(pd)} G_a}{r_0^3} = 0 \\ 3K_a A_a^{(pd)} - 4 \frac{B_a^{(pd)} G_a}{a^3} = 3K_m A_m^{(pd)} - 4 \frac{B_m^{(pd)} G_m}{a^3} \\ A_m^{(pd)} a + \frac{B_m^{(pd)}}{a^2} = A_a^{(pd)} a + \frac{B_a^{(pd)}}{a^2} \\ 3K_m A_m^{(pd)} - 4 \frac{B_m^{(pd)} G_m}{b^3} = S \end{cases} \quad (25)$$

which, after long but straightforward algebraic manipulations, further accounting for $b \gg r_0$ and $K_p \gg K_m, K_a$, gives:

$$\begin{aligned} A_a^{(pd)} &= \frac{\sigma_{cr} \zeta}{3K_p} \frac{G_a(4G_m + 3K_m)}{G_a(4G_m + 3K_a) - 3(r_0/a)^3 K_a(G_a - G_m)} \\ B_a^{(pd)} &= \frac{\sigma_{cr} \zeta}{4K_p} \frac{K_a(4G_m + 3K_m)}{G_a(4G_m + 3K_a) - 3(r_0/a)^3 K_a(G_a - G_m)} r_0^3 \end{aligned} \quad (26)$$

where ζ is given by Eq. (23) and G_m and G_a are the matrix and interphase shear moduli, respectively.

Finally, the radial displacement field results:

$$\begin{aligned} u^a &= \frac{\sigma_{cr} \zeta}{K_p} \\ &\times \frac{(4G_m + 3K_m)}{G_a(4G_m + 3K_a) - 3(r_0/a)^3 K_a(G_a - G_m)} \left(\frac{G_a r}{3} + \frac{K_a r_0^3}{4 r^2} \right) \end{aligned} \quad (27)$$

7. Analytical solution for the critical debonding stress

Once all stress constants have been determined, it is possible to explicitly reconsider Eq. (2b) where now the only unknown variable is the debonding stress, σ_{cr} , which can be determined in closed form. The final solution, noting that $E_m = 2G_m(1 + v_m)$, is:

$$\sigma_{cr} \cong \sqrt{\frac{4\gamma}{r_0} \frac{E_m}{1 + v_m} \sqrt{\frac{\chi(4 + \xi) - \xi(\chi - 1)(r_0/a)^3}{4 + \xi + 4(\chi - 1)(r_0/a)^3}}} \quad (28)$$

where $\chi = G_a/G_m$ and $\xi = 3K_a/G_m$ are two normalised elastic parameters. It is worth noting that σ_{cr} depends not only on the matrix and nanoparticle properties, but also on those of the interphase; moreover the size effect is accounted for through the radius of the nanoparticle as well as through the nanoparticle radius to the interphase radius ratio, r_0/a .

Based on the general solution given by Eq. (28) it is also possible to determine the limit values which might be representative of special material configurations.

The debonding stress can be thought of as not influenced by the interphase zone if one of the two following conditions is verified:

- the elastic properties of the interphase zone are not significantly different from those of the matrix ($\chi \rightarrow 1$);
- the interphase zone extension is negligible with respect to the nanoparticle size ($a/r_0 \rightarrow 1$).

Indeed it is evident that, as one of the above-mentioned conditions is verified, Eq. (28) simplifies as follows:

$$\sigma_{cr} \cong \sqrt{\frac{4\gamma}{r_0} \frac{E_m}{(1 + v_m)}} \quad (29)$$

Note that Eq. (29) completely disregards the presence of an interphase zone and matches the solution already proposed by other authors [17,20] for a system constituted by matrix and nanoparticles only.

It is finally worth noting that when the interphase size is much greater than the particle size, namely when $r_0/a \rightarrow 0$, Eq. (28) simplifies as follows:

$$\sigma_{cr} \cong \sqrt{\frac{4\gamma}{r_0} \frac{E_m}{(1 + v_m)}} \sqrt{\chi} \cong \sqrt{\frac{4\gamma}{r_0} \frac{E_a}{1 + v_a}} \quad (30)$$

Eq. (30) matches Eq. (29) when matrix properties are changed for interphase properties and represents the asymptotic value to which the complete solution tends as the ratio a/r_0 becomes sufficiently high. This asymptote strictly depends on χ and is not influenced by ξ .

8. Results and discussion

The aim of this section is to clarify the range of applicability and to highlight, through examples, the most relevant features of the solution proposed in the previous section.

It is first worth noting that, since no size limitations have been formulated in the model, Eq. (28) can be applied both to nanosized and microsized particles.

Moreover, the major novelty of the present work, with respect to previous ones in the literature [17,20], lays on the fact that Eq. (28) explicitly considers the effect of an interphase zone surrounding the nanoparticle, which might be characterised by physical properties different from those of the matrix. It is then interesting to quantify the effects of the interphase properties and size on the critical value of the debonding stress. To this end, Figs. 3–5 show a comparison between the results obtained on the basis of Eq. (28),

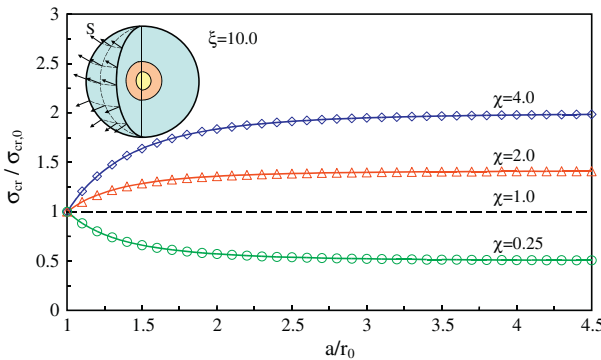


Fig. 3. Normalised debonding stress versus the a/r_0 ratio, according to Eq. (28). $\xi = 10$; different values of parameter χ . $\sigma_{cr,0}$ denotes the value for the debonding stress evaluated by disregarding the presence of the interphase zone, Eq. (29).

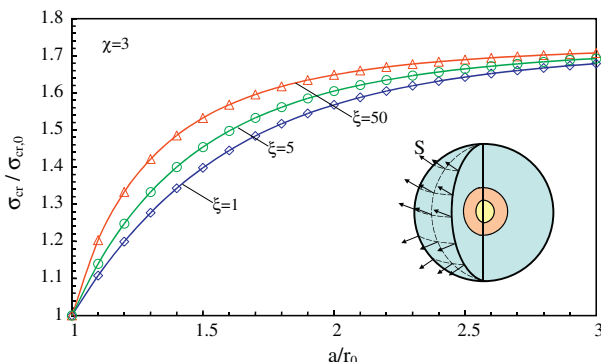


Fig. 4. Normalised debonding stress versus the a/r_0 ratio, according to Eq. (28). $\chi = 3$; different values of parameter ξ . $\sigma_{cr,0}$ denotes the value for the debonding stress evaluated by disregarding the presence of the interphase zone, Eq. (29).

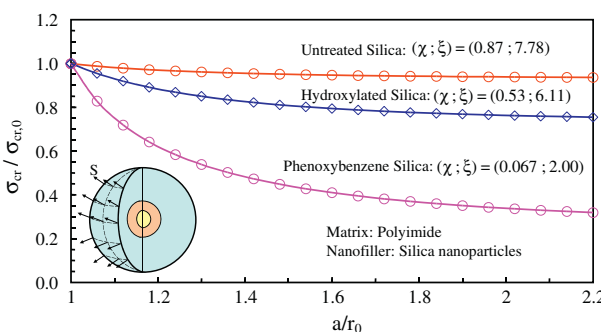


Fig. 5. Normalised debonding stress versus the a/r_0 ratio, according to Eq. (28). Different values of parameters χ and ξ representing different types of functionalisation (data taken from Odegard et al. [10]). $\sigma_{cr,0}$ denotes the value for the debonding stress evaluated by disregarding the presence of the interphase zone, Eq. (29).

which considers different matrix and interphase properties and different values of the interphase to nanoparticle radius-ratio, and Eq. (29) [17,22].

In particular, Fig. 3 highlights that the effect of the interphase on debonding stress strictly depends on the ratio between the interphase and the matrix shear moduli, χ . It is worth noting that, when the shear modulus of the matrix is greater than that of the interphase ($\chi < 1$), debonding stress decreases compared to the Chen et al. solution [17] while, for stiffer interphases ($\chi > 1$), the debonding stress increases. It is also evident that, either for stiffer or softer interphases, the asymptotic value represented by

Table 1

Elastic properties of the polyimide matrix/silica nanoparticle system used in Figs. 5 and 6. Properties are taken from Ref. [10] and were computed by means of molecular dynamics simulations.

Polyimide matrix	E_m	4.20	(GPa)
	G_m	1.50	
Interphase	Thickness t	1.2	(nm)
Phenoxybenzene Silica	G_a	0.10	(GPa)
	K_a	1.00	
Hydroxylated Silica	G_a	0.80	(GPa)
	K_a	3.06	
Untreated Silica	G_a	1.30	(GPa)
	K_a	3.89	

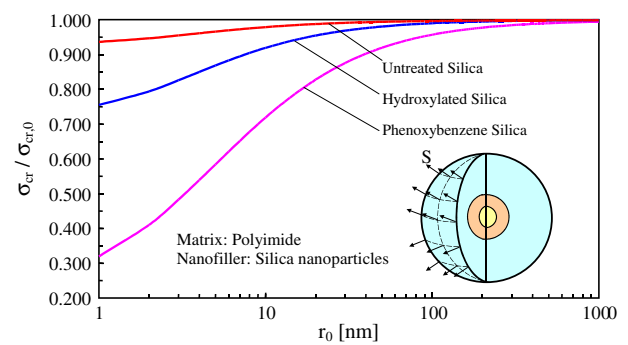


Fig. 6. Normalised debonding stress versus the nanoparticle size, r_0 , according to Eq. (28). The interphase thickness, t , is assumed to be independent of the particle size. Different types of functionalisation (data taken from Odegard et al. [10]). $\sigma_{cr,0}$ denotes the value for the debonding stress evaluated by disregarding the presence of the interphase zone, Eq. (29).

Eq. (30) is rapidly reached and there are no significant variations of the debonding stress for a/r_0 values greater than 2.

Fig. 4 highlights the effect of the parameter ξ on the solution. It is evident that this parameter has only a slight influence: varying ξ from 1 to 50 the maximum difference is within 30%. Moreover, it is worth noting that its influence is limited to a/r_0 ratios smaller than 3, while the asymptotic value depends only on parameter χ .

Fig. 5 shows the result of the application of the model to data taken from the literature [10]. In this case, the non-dimensional stress ratio is plotted versus the normalized radial extension of the interphase considering the elastic properties computed by Odegard and co-workers in Ref. [10]. All the necessary details are listed in Table 1.

It has to be noted that the use of different surface treatments results in different elastic properties for the interphase (see Table 1). Accordingly, the model gives a different debonding stress not only depending on the matrix mechanical properties but also on the surfactants used. This result is shown in Fig. 5, where it is evident that the debonding stress is affected by the surface treatment depending also on the radial extension ratio a/r_0 . In particular, for $a/r_0 = 2$, which can be considered a representative value as suggested in [10], Eq. (28) gives a value 20% lower (hydroxylated silica) and 60% lower (phenoxybenzene silica) than that obtained from Chen's model, which is interphase independent [17].

It is finally interesting to see which is the size range of particles where the present model differs from previous analyses already carried out in the literature [17]. Fig. 6 shows the normalized critical debonding stress, estimated through Eq. (28), of three silica nanoparticle/polyimide composites as a function of the particle size, r_0 . The elastic properties are according to those computed by Odegard and co-workers in Ref. [10] (see Table 1). A large range of particle radii, from 1 nm to 1 μ m, has been considered. However,

it is evident that for radii greater than 100 nm, the result matches that predicted by Chen's model, Eq. (29), as one may guess in view of the limited influence of the thin interphase. The different interphase properties, resulting from different surface functionalizers, have, instead, a significant effect on the debonding stress for nanoparticle radii below 50 nm. Obviously this result might change from case to case, depending on the system under investigation (matrix, nanoparticle and surfactants used).

9. Conclusions

In this work a closed form expression for the critical debonding stress accounting for the existence of an interphase zone between the nanoparticle and the matrix has been proposed. In more details:

- the problem has been formulated and solved by considering a nanoparticle of radius r_0 surrounded by a spherical interphase of radius a ;
- the expression for the critical debonding stress has been determined within the frame of the Finite Fracture Mechanics. Stress and displacement fields at incipient debonding and post debonding has taken place has been determined within the Cauchy Continuum Theory;
- since no size limitations have been formulated on the hypotheses, the new solution can be applied both to nanosized and microsized particles;
- the solution quantifies the role played by the properties and the size of the interphase zone. It has been shown that as different functionalizers lead to different elastic properties of the interphase, the debonding stress is affected by the surface treatment depending on the radial extension ratio a/r_0 . For $a/r_0 = 2$ Eq. (28) gives a value 20% lower (hydroxylated silica) and 60% lower (phenoxybenzene silica) than that obtained from Chen et al. model, Eq. (29), which is interphase independent [17];
- Finally, with reference to the silica nanoparticle/polyimide composites studied in [10], it has been shown that the different interphase properties, resulting from different surface functionalizers, have a significant effect on the debonding stress for nanoparticle radii below 50 nm.

Acknowledgements

The activity described in this paper was carried out in the frame of the PRIN national project “Improvement of the mechanical properties of polymeric composite laminates by matrix nanomodification” (20075939JY) financially supported by the Italian Ministry of Research and University.

The financial support to the activity by Veneto Nanotech, the Italian Cluster of Nanotechnology (Padova, Italy), is also greatly acknowledged.

Appendix A

Let us consider the system shown in Fig. 1. At incipient debonding, the Global Stress Concentration Tensor (GSCT) can be used to link the average stress tensor in the nanoparticle, σ , and the stress tensor in the overall composite, S , according to the following expression:

$$\sigma = H : S \quad (\text{A.1})$$

H is a fourth order isotropic tensor; in general such a tensor can be decoupled into a hydrostatic (spherical) component and a deviatoric component [31]:

$$H = H_h I_h + H_d I_d \quad (\text{A.2})$$

where I_h and I_d can be written as:

$$\begin{aligned} I_{h,(ijkl)} &= \frac{1}{3} \delta_{ij} \delta_{kl} \\ I_{d,(ijkl)} &= \frac{1}{2} \left(\delta_{ik} \delta_{jl} + \delta_{il} \delta_{jk} - \frac{2}{3} \delta_{ij} \delta_{kl} \right) \end{aligned} \quad (\text{A.3})$$

δ is the Kronecker delta and H_h and H_d are constants.

Equivalently, Eq. (A.2) can be re-written in the following form [31]:

$$H = (H_h, H_d) \quad (\text{A.4})$$

Then, according to Eq. (A.4), and accounting for the spherical symmetry of the problem, Eq. (A.1) can be re-written as:

$$(\sigma_{cr}, 0) = (H_h, H_d) \times (S, 0) \quad (\text{A.5})$$

Finally, considering only the hydrostatic component of Eq. (A.5), it results:

$$\sigma_{cr} = H_h S \quad (\text{A.6})$$

or, equivalently:

$$S = C_h \sigma_{cr} \quad (\text{A.7})$$

where C_h is then the reciprocal of the hydrostatic components of the Global Stress Concentration Tensor.

References

- [1] Wetzel B, Haupert F, Zhang MQ. Epoxy nanocomposites with high mechanical and tribological performance. Compos Sci Technol 2003;63:2055–67.
- [2] Thostenson ET, Li C, Chou TW. Nanocomposites in context. Compos Sci Technol 2005;65:491–516.
- [3] Wichmann MHG, Sumfleth J, Gojny FH, Quaresimin M, Fiedler B, Schulte K. Glass fibre-reinforced composites with enhanced mechanical and electrical properties – benefits and limitations of a nanoparticle-modified matrix. Eng Fract Mech 2006;73:2346–59.
- [4] Fiedler B, Gojny FH, Wichmann MHG, Nolte MCM, Schulte K. Fundamental aspects of nano-reinforced composites. Compos Sci Technol 2006;66:3115–31.
- [5] Quaresimin M, Varley RJ. Understanding the effect of nanomodifier addition upon the properties of fibre reinforced laminates. Compos Sci Technol 2008;68:718–26.
- [6] Ma J, Mo M-S, Du X-S, Rosso P, Friedrich K, Kuan H-C. Effect of inorganic nanoparticles on mechanical property, fracture toughness and toughening mechanism of two epoxy systems. Polymer 2008;49:3510–23.
- [7] Thostenson ET, Chou TW. On the elastic properties of carbon nanotube-based composites: modeling and characterization. J Phys D 2003;36:573–82.
- [8] Luo JJ, Daniel IM. Characterization and modeling of mechanical behavior of polymer/clay nanocomposites. Compos Sci Technol 2003;63:1607–16.
- [9] Smith JS, Bedrov D, Smith GD. A molecular dynamics simulation study of nanoparticle interactions in a model polymer-nanoparticle composite. Compos Sci Technol 2003;63:1599–605.
- [10] Odegard GM, Clancy TC, Gates TS. Modeling of mechanical properties of nanoparticle/polymer composites. Polymer 2005;46:553–62.
- [11] Scoccia G, Posocco P, Danani A, Prici S, Fermeglia M. To the nanoscale and beyond! Multiscale molecular modeling of polymer-clay nanocomposites. Fluid Phase Equilib 2007;261:366–74.
- [12] Fermeglia M, Prici S. Multiscale modeling for polymer systems of industrial interest. Progr Org Coat 2007;58:187–99.
- [13] Yu S, Yang S, Cho M. Multi-scale modeling of cross-linked epoxy nanocomposites. Polymer 2009;50:945–52.
- [14] Wetzel B, Rosso P, Haupert F, Friedrich K. Epoxy nanocomposites – fracture and toughening mechanisms. Eng Fract Mech 2006;73:2375–98.
- [15] Johnsen BB, Kinloch AJ, Mohammaed RD, Taylor AC, Sprenger S. Toughening mechanisms of nanoparticle-modified epoxy polymers. Polymer 2007;48:530–41.
- [16] Zhao S, Schadler LS, Duncan R, Hillborg H, Aulett T. Mechanisms leading to improved mechanical performance in nanoscale alumina filled epoxy. Compos Sci Technol 2008;68:2965–75.
- [17] Chen JK, Huang ZP, Zhu J. Size effect of particles on the damage dissipation in nanocomposites. Compos Sci Technol 2007;14:2990–6.
- [18] Lauke B. On the effect of particle size on fracture toughness of polymer composites. Compos Sci Technol 2008;68:3365–72.
- [19] Lauke B. Determination of adhesion strength between a coated particle and polymer matrix. Compos Sci Technol 2006;66:3153–60.
- [20] Williams JG. Particle toughening of polymers by plastic void growth. Compos Sci Technol 2010;70:885–91.

- [21] Nicholson DW. On the detachment of a rigid inclusion from an elastic matrix. *J Adhes* 1979;10:255–60.
- [22] Gent AN. Detachment of an elastic matrix from a rigid spherical inclusion. *J Mater Sci* 1980;15:2884–8.
- [23] Wichmann MHG, Cascione M, Fiedler B, Quaresimin M, Schulte K. Influence of surface treatment on mechanical behaviour of fumed silica/epoxy resin nanocomposites. *Compos Interfaces* 2006;13:699–715.
- [24] Tian L, Rajapakse RKND. Elastic field of an isotropic matrix with a nanoscale elliptical inhomogeneity. *Int J Solids Struct* 2007;44:7988–8005.
- [25] Ajayan PM, Schadler LS, Braun PV. Nanocomposite science and technology. Wiley-VCH; 2003. ISBN:3527303596.
- [26] Sevostianov I, Kachanov M. Effect of interphase layers on the overall elastic and conductive properties of matrix composites. Applications nanosize inclusion. *Int J Solids Struct* 2007;44:1304–15.
- [27] Zammarano M, Maupin PH, Sung LP, Gilman JW, McCarthy ED, Kim YS, et al. Revealing the interface in polymer nanocomposites. *ACS NANO* 2011;5:3391–9.
- [28] Leguillon D. Strength or toughness? A criterion for crack onset at a notch. *Eur J Mech A/Solid* 2002;21:61–72.
- [29] Gross D, Seelig T. Fracture mechanics: with an introduction to micromechanics. Springer; 2006. p. 30.
- [30] Boutaleb S, Zaïri F, Mesbah A, Naït-Abdelaziz M, Gloaguen JM, Boukharouba T, et al. Micromechanics-based modelling of stiffness and yield stress for silica/polymer nanocomposites. *Int J Solids Struct* 2009;46:1716–26.
- [31] Qu J, Cherkaoi M. Fundamentals of micromechanics of solid. Hoboken, New Jersey: John Wiley & Sons, Inc; 2006.